European Journal of Pharmaceutics and Biopharmaceutics 76 (2010) 275–281

Contents lists available at ScienceDirect

European Journal of Pharmaceutics and Biopharmaceutics

journal homepage: www.elsevier.com/locate/ejpb

Research paper

Enhanced topical delivery and anti-inflammatory activity of methotrexate from an activated nanogel

Gillian S. Leslie Singka [a], Nor Abu Samah [a], Mohd H. Zulfakar [a], Aysu Yurdasiper [b], Charles M. Heard [a,*]

[a] Welsh School of Pharmacy, Cardiff University, CF10 3NB, UK
[b] Faculty of Pharmacy, Ege University, 35100 Bornova, Izmir, Turkey

ARTICLE INFO

Article history:
Received 8 February 2010
Accepted in revised form 23 June 2010
Available online 30 June 2010

Keywords:
pNIPAM
Nanogel
Methotrexate
Topical delivery
Inflammation

ABSTRACT

This work examined the effect of sodium carbonate (Na_2CO_3) on the topical delivery of methotrexate (MTX) from a loaded nanogel *in vitro* and the modulation of prostaglandin E_2 (PGE_2) production in skin *ex vivo*. A nanogel based on co-polymerised *N*-isopropylacrylamide (NIPAM) and butylacrylate (BA) was synthesized, characterized and loaded with MTX. Finite doses were then applied to excised porcine epidermal membranes mounted in Franz diffusion cells, followed by the addition of saturated aqueous Na_2CO_3. For comparison, the addition of half-saturated Na_2CO_3 was examined along with loaded nanogel alone. The same treatments were applied to Silastic membrane and full-thickness porcine ear skin *ex vivo*, which was then treated with radioimmunoprecipitation buffer and probed for levels of PGE_2 using a commercial enzyme immunoassay kit. The MTX-loaded nanogel, which demonstrated de-swelling by 7% over the range 25–37 °C, provided a MTX flux of 1.4 ± 0.3 ng cm^{-2} h^{-1}; this increased to 3.1 ± 0.22 ng cm^{-2} h^{-1} upon the addition of saturated aqueous Na_2CO_3 ($p < 0.05$). Lag times were 6 and ~0 h, respectively. Similar results were obtained using half-saturated aqueous Na_2CO_3. No permeation was detected across Silastic membrane. PGE_2 levels for water (control) and saturated aqueous Na_2CO_3 were similar, but reduced by 33% when the MTX-loaded nanogel was applied, and by 57% when this was followed by the application of saturated aqueous Na_2CO_3 ($p < 0.01$). A novel mechanism is proposed whereby the change in temperature experienced by the nanogel as it penetrated skin induced de-swelling and expulsion of MTX in situ. The added Na_2CO_3 lead to further solubilisation and MTX release, hence increasing the concentration gradient, flux and reducing PGE_2 production.

1. Introduction

Methotrexate (MTX) is a potent immunomodulating drug indicated as second-line treatment for severe psoriasis and, currently, only oral forms are available with a weekly recommended dosage of between 10 and 25 mg. Despite its efficacy, the use of MTX is greatly limited due to its toxicity, and one way to limit the systemic toxicity is by formulating MTX into a topical product. The drug has been the subject of much research in this respect [1–4], although a product has yet to be marketed. One reason for generally poor clinical effect is insufficient percutaneous penetration of MTX to the basal layer of epidermis in order to exert its pharmacological action.

This work concerns a novel topical drug delivery system for MTX involving nanogels, which are colloidal, cross-linked particles with a size range between 100 nm and 1 μm [5–7] and which possess the property of swelling in appropriate solvents [8]. The stimulus-responsive nature of nanogels is attractive and has potential uses in many applications, including pharmaceuticals [8]. Depending on the chemical nature of the monomers used, nanogels undergo volume-phase transition in response to stimuli, such as temperature [9], ionic strength [10] and solvent type [11]. A range of monomers is available that can be used to produce nanogels, e.g. styrene, methyl methacrylate and divinylbenzene [6]. Biodegradable, pH-responsive chitosan nanogels have been examined as a means to achieve rapid cellular internalisation of MTX [12]. However, due to its thermo-responsive behaviour and unique feature of undergoing lattice collapse close to the human body temperature [13], the most studied monomer in the pharmaceutical area is *N*-isopropylacrylamide (NIPAM), which undergoes collapse (has a lower critical solution temperature, LCST) at 32–34 °C, depending on the chemical environment [14].

The major influence on the swelling/collapsing behaviour of polyNIPAM-based nanogels is the balance between attractive and repulsive forces acting internally. At temperatures below the LCST the linear polymer is highly solvated due to the extensive formation of hydrogen bonds between the solvent and the amide side chains of the polymer, causing the polymer to coil randomly. But as temperature exceeds the LCST, hydrogen bonds dissociate and the polymer shrinks, or de-swells, on the entropically favoured

* Corresponding author. Tel.: +44 029 2087 5819; fax: +44 029 2087 4149.
E-mail address: heard@cf.ac.uk (C.M. Heard).

0939-6411/$ - see front matter © 2010 Elsevier B.V. All rights reserved.
doi:10.1016/j.ejpb.2010.06.014

release of water from the polymer interior, with the polymer now existing in a globular form. When the polymer chains are cross-linked into a network by a cross-linker, the responsivity appears as a volume collapse followed by the expulsion of their contents. This transition temperature is called the volume phase transition temperature (VPTT). Generally, the VPTT is close to the LCST of the corresponding non cross-linked polymer solution. This temperature-induced behaviour, of absorbing solvated materials (e.g. a drug) under one set of conditions then release when environmental conditions change, can be utilised in drug delivery systems [13]. PolyNIPAM nanogels can also be made to be pH responsive through co-polymerisation with ionic monomers such as acrylic acid and methacrylic acid [6]. A recent observation suggested that the addition of a base (triethylamine) to a nanogel comprised of a co-polymer of NIPAM and non-ionic monomer butylacrylate (polyNIPAM-*co*-BA) produced significant enhancements in the topical delivery of naproxen across skin. However, the use of triethylamine was found to be unsuitable due to it being highly pro-inflammatory (unpublished data).

In the current study, a polyNIPAM-co-BA nanogel was prepared and characterized, before being loaded with MTX. The delivery of MTX was then determined from the nanogel applied to heat-separated epidermal membranes *in vitro*, and the effect of base sodium carbonate (Na_2CO_3) determined – Na_2CO_3 is widely used in the cosmetic industry as a pH regulator and is certified as safe for use by the Cosmetic Ingredient Review (CIR) Expert Panel [15]. The same treatments were applied to Silastic membrane and *ex vivo* porcine skin, where the skin was assayed for the key inflammation mediator, prostaglandin E_2 (PGE_2).

2. Materials and methods

2.1. Materials

N-isopropylacrylamide (NIPAM), butylacrylate (BA), potassium persulfate (PP), sodium carbonate (Na_2CO_3) anhydrous, sodium hydroxide (NaOH, 1 N), concentrated hydrochloric acid (HCl), HPLC-grade methanol, glass wool and filter paper were all purchased from Fisher Scientific (Loughborough, UK). Radioimmunoprecipitation (RIPA) buffer, *N*,*N*′-methylenebis-acrylamide (BIS), Hank's balanced salt, potassium phosphate monobasic, phosphate-buffered saline solution (PBS) were all purchased from Sigma–Aldrich Company (Poole, UK). Methotrexate (MTX) was obtained from Heumann PCS GmBH (Feucht, Germany). The 'Cayman prostaglandin E_2 EIA kit – monoclonal' was purchased from Cayman Europe (Tallinn, Estonia). Silicone membrane (75 μm thickness) was obtained from Dow Corning Company (Seneffe, Belgium). Porcine ears were obtained from a local abattoir prior to steam cleaning and immersed in iced Hank's buffer upon excision

2.2. Nanogel synthesis

Poly(NIPAM-*co*-BA) nanogel was synthesized using a surfactant-free emulsion polymerisation method. NIPAM, BIS (cross-linker) and PP (initiator) were used in the ratio 91:7:2, respectively. Briefly, NIPAM, BIS and de-ionised water were added together in a beaker and stirred for ~15 min on a magnetic stirrer plate. This dissolved solution was continuously stirred in a 250-mL three-neck, round-bottom flask equipped with a magnetic stirrer and immersed in a water bath heated to the polymerisation temperature of ~70 °C. The flask was continually purged with nitrogen gas to maintain anoxic conditions. BA was added at a concentration of 7.5% w/w to the base monomer polyNIPAM approximately 15 min prior to the addition of the initiator. The polyNIPAM nanogel was hydrophobically modified using BA in order to modify its thermosensitive property. After being stabilized at ~70 °C, the monomer solution was initiated by addition of a hot predissolved persulfate initiator (made up beforehand in 100-mL of de-ionised water). Polymerisation was allowed to proceed for 6 h under continuous 300 rpm mixing. Afterwards, the nanogel suspension was cooled overnight under constant stirring (300 rpm). The mixture was then filtered by a combination of glass wool and filter paper. The crude nanogel product was subsequently purified by 5× centrifugation steps (Beckman Coulter J25), 1 h cycle @ 15 °C, 13,000*g*. PolyNIPAM nanogel is hydrophilic at room temperature; however, the presence of a cross-linker (BIS) prevents the nanogel from dissolving in water at temperatures < LCST [16,17]. The cross-linker restricts the extent of polymer swelling [18].

2.3. PolyNIPAM-co-BA nanogel characterization

2.3.1. Transmission electron microscopy (TEM)

TEM micrographs of the nanogel particles were obtained using a Phillips EM 208 TEM operated at 80 kV. Freeze-dried nanogels were re-suspended in de-ionised water at a concentration of 0.5% w/v and 10 μL transferred by a pipette onto Pioloform™-coated copper grid supports. The water on the grid was removed via blotting with a filter paper from the below, and the grid air-dried at the ambient temperature prior to microscopic observation. Quantitative microscopy measurement of TEM micrographs were performed using an online digital image processing program, ImageJ (Image processing and analysis in JAVA) version 1.43c (National Institute of Health, USA).

2.3.2. Particle size distribution

The purified nanogel particles were characterized at ambient temperature using a laser diffraction system (Malvern Mastersizer 2000™). The analysis was carried out on 0.1% w/v nanogel dispersion in de-ionised (temperature-dependent study) or pH-adjusted water (pH-dependent study). For each replicate, a new pipette was used to apply the sample into the instrument until the laser obscuration reading reached an approximate value of 10%. Each sample was analysed in triplicate ($n = 3$). Nanogel dispersions were stored at different temperatures: 4 °C (refrigerator), 25 °C (room temperature), 32 °C (average skin surface temperature), 37 °C (physiological temperature) and 60 °C, allowing at least 1 h for temperature equilibrium. The response of nanogels to pH was also investigated. Solutions of five different pH values (~pH 3, 5.8, 7, 9, and 12) were prepared through the drop-wise addition of either a HCl (0.1 M) or NaOH (0.1 M), monitored using a standard pH meter. Nanogel dispersions of 0.1 % w/v were prepared by mixing the freeze-dried nanogels in the solutions of variable pH using a laboratory flask shaker (Stuart™ Flask Shaker - SF1 *Bibby Scientific Ltd.,* Stone, UK) for 30 min. The dispersions were left to equilibrate at room temperature for a further 30 min prior to analysis using a Malvern Mastersizer 2000™. The measurements were performed at room temperature ($n = 3$).

The fundamental size distribution derived by this technique was volume-based and expressed in terms of the volume of equivalent spheres ($D_{N\%}$) and weighted mean of the volume distribution. As the laser diffraction system was used for the analysis, two values that would give an equivalent determination of particle polydispersity are uniformity (how symmetrical the distribution is around the median point) and span values (the width of the distribution). The span value is defined as below:

$$\text{Span} = \frac{D_{90\%} - D_{10\%}}{D_{50\%}} \quad (1)$$

where $D_{N\%}$ ($N = 10, 50, 90$) means that the volume percentage of particles with diameters up to $D_{N\%}$ equals to *N*%. The smaller the span value is, the narrower the size distribution.

2.4. Loading of nanogel with MTX

To enable high MTX loading into blank poly(NIPAM-*co*-BA) nanogel, it was important that MTX was in solution at high concentration, although MTX is generally known to be poorly soluble across a range of regular solvents. Various solvents were examined including dimethyl sulfoxide (DMSO), to poor effect. However, by trial and error, a dissolution method for MTX was developed in-house. First, MTX was suspended in de-ionised water and the pH adjusted by the dropwise addition of 1 N NaOH. The yellow suspension clarified once pH 12 was reached, the pH was then readjusted back to neutral by the dropwise addition of HCl, with the MTX remaining in solution. The MTX solution was then added to the purified blank nanogel in equal volumes and placed in an ultrasonic bath for 1 h, before being left overnight at room temperature. The mixture was then centrifuged as described earlier, the supernatant was decanted and discarded, and the precipitate retained for use.

2.5. Preparation of saturated aqueous sodium carbonate (Na_2CO_3)

A saturated solution of Na_2CO_3 was prepared by adding excess into 2 mL of de-ionised water in an Eppendorf tube until no further dissolution was observed. The vial was loaded on a rotary blood cell mixer and left to equilibrate overnight at room temperature. Later, the tube was centrifuged at 6000 rpm for 10 min, and the supernatant decanted and used immediately. A half-saturated solution was prepared from this saturated solution, by a 50:50 dilution using de-ionised water.

2.6. Preparation of membranes

Porcine skin was used because it is very similar in structure to the human skin, with permeability values close to that of the human skin [19,20]. As the site of action of MTX is the viable epidermis, the appropriate model membrane for drug delivery is heat-separated epidermis and these were prepared by an established technique. Porcine ears were cleaned under running water and the skin excised from the dorsal side by blunt dissection, prior to being cut into sections of approximately 3 × 3 cm and immersed in water heated to 60 °C for approximately 1 min, before gently peeling off the epidermis with the aid of forceps. For the bioassay for PGE_2, full-thickness skin membranes were used in order to retain metabolic activity, with the membranes continually bathed in Hank's buffer. Silastic sheet was washed under running water before being cut into 3 × 3 cm sections and soaked in receptor phase overnight.

2.7. In vitro permeation studies

The skin or Silastic membrane was mounted onto the pre-greased receptor compartment of a Franz diffusion cell with the *stratum corneum* facing upwards. The nominal diffusion area of the Franz cell was 0.95 cm^2 and had a receptor volume of 4.3 mL. Magnetic stirrers were placed into the receptor compartment to ensure uniform distribution of permeating solute for later sampling. The donor compartments were clamped firmly into place and the receptor phases filled with degassed PBS – which provided an adequate sink for MTX. The complete cells were then placed on a submersible magnetic stirring plate (Variomag, Daytona Beach) set up in a water bath maintained at 37 °C and left to equilibrate for 30 min. Finite doses of nanogel were applied using a blunt glass rod which was dipped momentarily into the MTX-loaded nanogel and then massaged gently onto the membrane to ensure uniform distribution without tearing the skin. Refining this method, the approximate weight of nanogel dosed was found to be consistently 0.1 g. Both the sampling arm and donor compartments were occluded. Three dosing procedures were used:

(a) MTX nanogel alone.
(b) MTX nanogel followed by 25 μL saturated aqueous Na_2CO_3.
(c) MTX nanogel followed by 25 μL 0.5× saturated aqueous Na_2CO_3 (not Silastic).

Sampling was carried out over a period of 12 h, with the entire receptor phases being removed using Pasteur pipettes and replaced with fresh, pre-warmed PBS. Each cell had a dedicated pipette to avoid cross-contamination. A 1-mL sample of the removed receptor solutions was retained for analysis.

2.8. Quantitative analysis

MTX in the receptor-phase samples was analysed by reversed-phase liquid chromatography using an Agilent 1100 series automated system with Chemstation software. The HPLC method was developed in-house: Luna C18 ODS 150 × 4.6 mm, 5 μm column (Phenomenex, Macclesfield, UK), mobile phase of 3:1 potassium phosphate buffer (0.1 M, pH 6.5)/methanol over 15 min with flow rate set at 1 mL min^{-1}. Sample injection volume was 20 μL and detection was by UV at λ = 305 nm, with a resultant MTX retention time of 9 min. For calibration, a stock solution of MTX (500 μg mL^{-1}) was prepared in PBS, and a standard calibration curve was obtained over the range of 4–500 μg mL^{-1}. Excellent linearity was achieved as evidenced by a R^2 of 1.000, with a limit of detection of 7.27 ng mL^{-1}. Cumulative amount of MTX permeated per unit area (mass cm^{-2}) was plotted against time (h), with lag time and steady state flux (J_{SS}) determined by standard methods. Cumulative permeation after 12 h (Q_{12}) is also reported.

2.9. Determination of PGE_2 in porcine skin ex vivo

MTX is known to be anti-inflammatory, and one way of observing this effect is by determining modulation in levels of the inflammation marker, PGE_2 [21]. Meanwhile, this bioassay can also indirectly indicate the extent of MTX delivery into the skin, as any reduction in PGE_2 must be a consequence of MTX activity on the viable keratinocytes. To facilitate extended skin viability and thus maintain skin metabolism and any arachidonic acid activities, the freshly excised porcine ears were immersed in iced Hank's buffer during transportation from the abattoir to the laboratory – the skin was used within 3 h of slaughter. The full-thickness skin was cut into approximately 2 × 2 cm sections and placed in Hanks balance salt, then mounted into Franz diffusion cells, as described earlier. The skin was dosed in triplicate with one of four groups according to dosing types: MTX nanogel alone, MTX nanogel with base added, with 20 μL saturated Na_2CO_3, 20 μL de-ionised water. The receptor phase was degassed Hank's buffer. After 6 h, the diffusion cells were dismantled and the skin washed to remove residual doses, then cut into small pieces using a scalpel and immersed in RIPA buffer to break up the tissues and release metabolites with the aid of an ultrasonic bath. PGE_2 levels were then determined using the enzyme immunoassay kit in accordance with the instructions supplied, followed by colorimetric determination at 412 nm.

2.10. Statistical analysis

The nanogel characterization data were analyzed using Excel 2007 (Microsoft Office, Microsoft Inc., US) and expressed as a mean ± standard deviation (S.D.). The MTX delivery and PGE_2 modulation data were analysed statistically using the unpaired, two-tailed *t*-test with Welch correction. The test was conducted with Instat 3

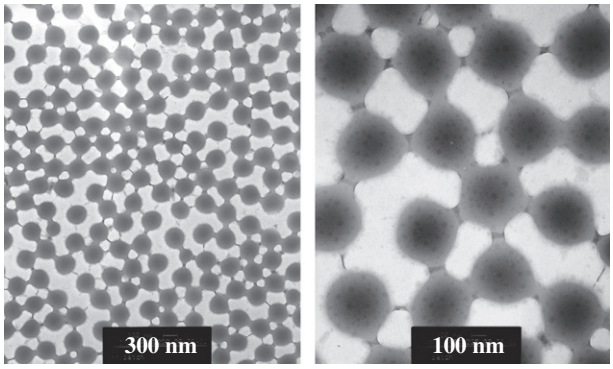

Fig. 1. Transmission electron micrographs of poly(NIPAM-*co*-BA). Scale bar: left 300 nm, right 100 nm.

for Macintosh (Graphpad, California, USA). Confidence intervals were set at 95%, and $p < 0.05$ was defined as statistically significant.

3. Results and discussion

3.1. Characterization of blank polyNIPAM-co-BA

The two TEM images in Fig. 1 confirm that the nanogel particles were monodisperse by having uniform size and spherical shape. The images also serve to validate the purification step, by the absence of extraneous particulates. TEM allows visual assessment of the particles, but the samples need to be dried and viewed in a collapsed state. When a drop of dilute nanogel is placed on a TEM microscope grid, the swollen monodisperse particles are pulled by surface tension forces to form the two-dimensional ordered arrays. Further drying causes the latex particles to shrink and form disks of nanogels which remain in the original configuration. Particle size analysis was done on the nanogel micrographs, and it was found that the gel has an average particle size of 113.43 ± 7.06 nm in the dried state. Particle size analysis done by laser diffraction method (Malvern Mastersizer 2000™) showed that the gels had an average hydrodynamic particle size of ~150 nm at room temperature with a span value of 0.923 ± 0.035. There was ~23% of size increment compared to the dried size. The size in dry state is smaller than the hydrodynamic size due to the shrinking of the particles in drying process.

The blank nanogel was examined for pH-mediated particle size modulation. Fig. 2 shows the particle size distribution curves at five different pH values superimposed on each other, revealing the non-pH-responsive nature of the nanogel. On the other hand, Fig. 3 shows a trend in the hydrodynamic size of the blank nanogel at 4, 25, 32, 37 and 60 °C, whereby smaller (de-swollen) particle size is observed with increasing temperature. This volume transition was found to be reversible as noted previously [22].

In principle, nanogels should undergo volume collapse at a temperature close to body temperature and size decreasing with increase in temperature [23]. From a topical delivery perspective, the key interval is that between 25 and 37 °C signifying a typical storage temperature to bodily temperature, via 32 °C – the average surface skin temperature. Over this range, the nanogel underwent de-swelling by 11.5%, which was considered very significant (p, 0.0024). BA has previously been successfully used to reduce the VPTT of polyNIPAM nanogel to <32–35 °C, thus the current nanogel would be expected to demonstrate greater sensitivity (i.e. de-swelling) when in contact with the skin [24].

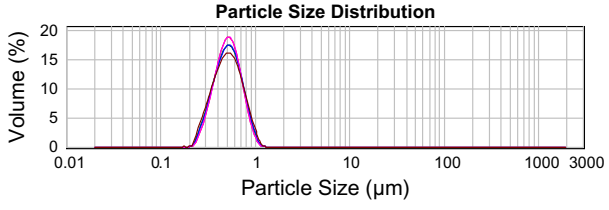

Fig. 2. The effect of pH on the particle size distribution of blank polyNIPAM-co-BA nanogel (pH 3, 5.8, 7, 9 and 12). Note particle size distribution is the same for each pH. (For interpretation of the references to colour in this figure legend, the reader is referred to the web version of this article.)

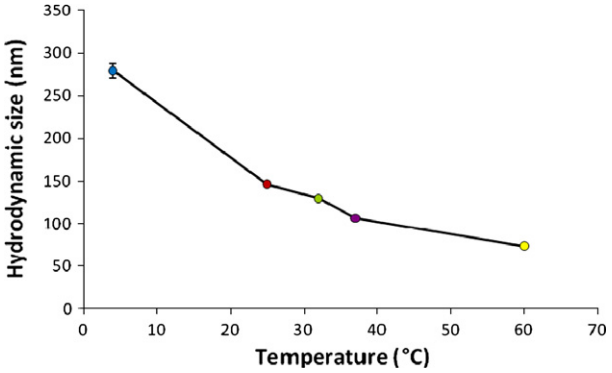

Temperature (°C)	Span	Uniformity
4	0.787 ± 0.029	0.171 ± 0.001
25	0.923 ± 0.035	0.182 ± 0.001
32	0.840 ±0.037	0.181 ± 0.003
37	0.989 ±0.005	0.184 ± 0.006
60	0.601 ±0.003	0.200 ± 0.011

Fig. 3. The effect of temperature on the particle size distribution of blank poly(NIPAM-*co*-BA) nanogel. Graphical data represents mean hydrodynamic size; span and uniformity values represent nanoparticle polydispersity ($n = 3 \pm$ S.D.). Note de-swelling with increasing temperature.

3.2. Preparation of MTX-loaded polyNIPAM-co-BA nanogel

At the end of the centrifugation step, an orange-coloured sediment product was isolated, with the decanted supernatant a noticeably lighter shade of orange relative to saturated solution prior to the loading step, indicating that the nanogel had successfully absorbed MTX. To determine the amount of MTX loaded into the nanogel, the supernatant obtained after centrifugation was assayed by HPLC. The difference in the average MTX concentration between the saturated solution (7.40 mg mL^{-1}) and the supernatant (5.04 mg mL^{-1}) was taken to be the amount loaded into the nanogel, i.e. 2.36 mg mL^{-1}. Since 2 mL of MTX was added to 2 g of the swollen nanogel, the amount of MTX encapsulated into the nanoparticles was 2.36 mg g^{-1}, providing a loading efficiency of 31.9%.

3.3. Permeation of MTX across heat-separated epidermal and Silastic membranes

Fig. 4 and Table 1 show that when loaded nanogel was applied alone, the permeation of MTX across the heat-separated membrane was less than the limit of detection until 6 h; after that time the flux was 1.4 ± 0.3 ng cm^{-2} h^{-1}. When the application of the loaded nanogel was followed by application of 25 μL of saturated aqueous Na_2CO_3 (≈480 mgmL^{-1} – pH12.64), lag time was reduced to approximately 0 h. The flux increased to 3.1 ± 0.22 ng cm^{-2} h^{-1}, and the Q_{12} increased to 44 ± 9.56 ng cm^{-2}. Both values were statistically significant relative to the control (p, 0.0001 and 0.0006, respectively). When the application of the loaded nanogel was followed by application of 25 μL of 0.5× saturated aqueous Na_2CO_3, lag time was again reduced to approaching 0 h. The flux was 2.6 ± 0.22 ng cm^{-2} h^{-1}, and the Q_{12} was 37 ± 2.14 ng cm^{-2}. Again,

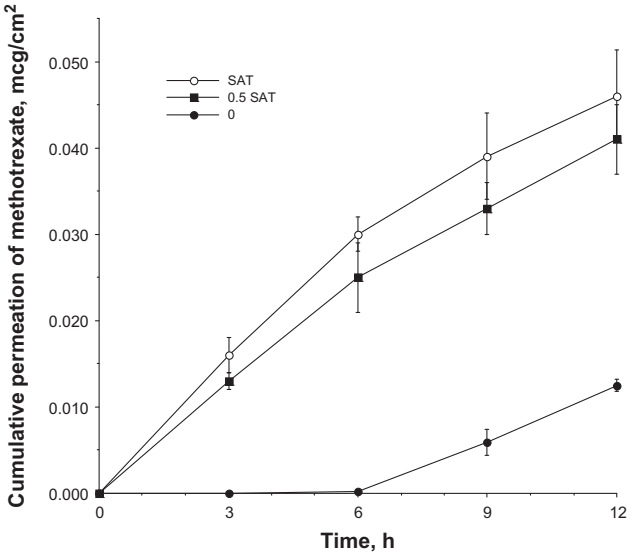

Fig. 4. Cumulative permeation of methotrexate across porcine ear skin from loaded poly(NIPAM-*co*-BA) nanogel. 0: no added Na_2CO_3, SAT: skin dosed with only 25 μL saturated aqueous Na_2CO_3, 0.5 SAT: skin dosed with only 25 μL half-saturated aqueous Na_2CO_3. ($n \geqslant 3 \pm$ SD).

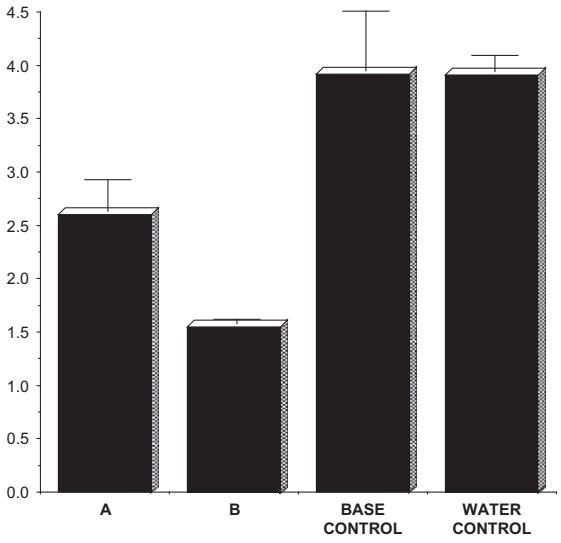

Fig. 5. Bar chart comparing the concentrations of PGE_2 in ng mL^{-1} from the different treatment groups: A = MTX-loaded nanogel, B = MTX-loaded nanogel followed by 25 μA saturated aqueous Na_2CO_3, base control = skin dosed with only 25 μL saturated aqueous Na_2CO_3, and control = skin dosed with de-ionised water. ($n = 3 \pm$ SD).

both values were statistically different to the control (p, 0.007 and 0.0001, respectively), and although there was an apparent trend for lower amounts, statistically these were the same as for the fully saturated Na_2CO_3 ($p > 0.05$).

The MTX-loaded nanogel alone was capable of delivering the drug, albeit with a relatively long lag/breakthrough time. However, for many therapeutic indications, a low lag time value is desirable in order to accelerate the onset of therapeutic activity. This was achieved by the co-administration of Na_2CO_3, which both increased flux and virtually eliminated breakthrough/lag time. As both half- and fully saturated Na_2CO_3 gave the same result, the enhancement process appears saturable.

When the same treatments were applied to Silastic membrane, no MTX was detected in the receptor phases over the 12 h period, regardless of whether Na_2CO_3 solution was added or not.

3.4. Modulation of skin PGE_2 levels

Enhanced delivery of MTX to skin would be expected to be reflected in modulated biological activity. Although principally a dihydrofolate reductase (DHFR) inhibitor, MTX has anti-inflammatory properties, and, in the current model, enhanced bioavailability in the viable epidermis would be expected to lead to increased uptake by keratinocytes and thus reduced production of PGE_2.

Fig. 5 shows that when dosed with a saturated solution of Na_2CO_3, the amount of PGE_2 found in the skin was 3.93 ng – virtually the same level (3.90 ng) was found following the application of water ($p > 0.05$). This was very encouraging as it demonstrated that Na_2CO_3 does not exert a pro-inflammatory effect. When the skin was dosed with MTX-loaded nanogel, a significant reduction (33%) in PGE_2 was observed (p, 0.0154). Furthermore, when the skin was dosed with MTX-loaded nanogel and followed by Na_2CO_3 solution, the reduction was even greater, by 60% relative to the water control (p, 0.0012). The effect on the PGE_2 levels of the added Na_2CO_3 compared to none was also significant (−57%) (p, 0.0052).

Fig. 5A supports the delivery data in Section 3.3 and demonstrates that the MTX-loaded nanogel was able to deliver the drug to the keratinocytes of the viable epidermis, as evidenced by the large reduction in PGE_2 present relative to the controls. However, the even greater (60%) reduction observed when Na_2CO_3 was co-administered (Fig. 5B) again reflects the transport data of Section 3.3, but with the additional proof of enhanced uptake by the keratinocytes.

As there was no difference between skin dosed with water of saturated Na_2CO_3 in terms of PGE_2 levels, it can be concluded that this solution had no pro-inflammatory effect when applied to skin. The probable explanation is that the very polar molecules of Na_2CO_3 did not penetrate appreciably into the skin. This further infers that whatever effect Na_2CO_3 had on the nanogel and MTX, the process did *not* occur within the viable epidermis.

3.5. Proposed mechanism

In establishing the delivery mechanism behind the observed data, there are two key facts. Firstly, the delivery and biological activity of MTX were both enhanced following the addition of Na_2CO_3 solution. Secondly, permeation of MTX and reduction of PGE_2 was observed even without the addition of Na_2CO_3. Dealing with the second point first, nanogels are known to be absorbed into skin, hence their use in the current work. By use of a glass rod, the nanogels were massaged into the skin, and assuming the absorption process was rapid, the nanogel would have experienced a significant increase in temperature once within the skin. As we know from Fig. 3, this would have been accompanied by a 7% decrease in

Table 1
Lag time, flux and cumulative permeation after 12 h data for MTX across the heat-separated epidermal membrane and total ($n \geqslant 3 \pm$ SD).

Dosing regimens	Lag time (h)	J_{SS} (ng cm^{-2} h^{-1})	Q_{12} (ng cm^{-2})
MTX-polyNIPAM-*co*-BA nanogel	6	1.4 ± 0.3	12.0 ± 1.60
MTX-polyNIPAM-*co*-BA nanogel followed by 25 μL saturated aqueous Na_2CO_3	~0	3.1 ± 0.22	44.0 ± 9.56
MTX-polyNIPAM-*co*-BA nanogel, followed by 25 μL 0.5× saturated aqueous Na_2CO_3	~0	2.6 ± 0.22	37.0 ± 2.14

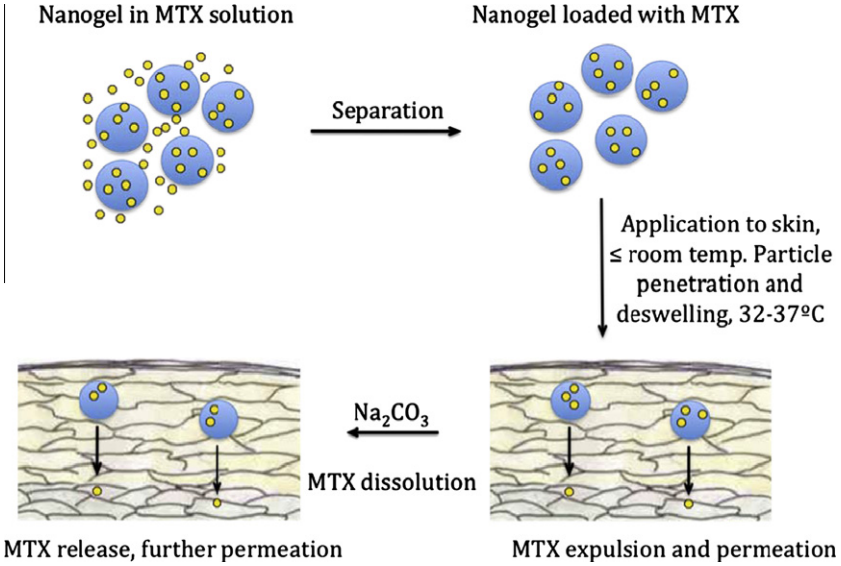

Fig. 6. Schematic illustration of proposed drug delivery mechanism.

particle size. Such de-swelling would act to expel MTX from the nanogel matrix *in situ*. The liberated MTX would then be able to diffuse through to the receptor phase and modulate COX-2 activity (reduce PGE_2 levels) within the keratinocytes.

As regards the addition of Na_2CO_3, pH-responsive nanogels have been reported in the literature, but these earlier works involved NIPAM and the ionic co-monomer e.g. acrylic acid [25]. The co-monomer used in the current investigation was BA, and the resulting nanogel demonstrated a lack of pH sensitivity (Fig. 2); therefore, the enhancement observed following the addition of the Na_2CO_3 could not have involved pH-mediated particle size modulation. One potential answer is that the increased pH, due to the addition of Na_2CO_3, facilitated the in situ solubilisation of the MTX (Section 2.4) and dissolution from within the nanoparticles already deposited within the skin. This would indicate localization beyond the *stratum corneum*, i.e. within the more hydrophilic viable epidermis. As a result, MTX molecules were able to diffuse more freely from the nanogel matrix, further increasing the concentration gradient, hence flux and biological activity.

Silastic membrane is a relatively simple matrix, lacking the complex architecture and biological activity of skin [26]. Undetectable levels of permeated MTX could reflect low permeability of the drug across this membrane. Alternatively, it could have been due to MTX nanoparticles failing to penetrate into the membrane, unlike skin where MTX was released in situ. Overall, the proposed mechanism can be summarized as in Fig. 6. Solubilisation of MTX by the Na_2CO_3 and release from the nanogel particle must have involved ionisation of carboxylic acid groups. The fluxes of ionised compounds are generally known to be low through the *stratum corneum* due to its lipophilic nature, which suggests the nanogel particles had penetrated as afar as the viable epidermis, which has a far more polar nature and therefore more conducive to the diffusion of ionised MTX.

Although we currently have no direct evidence for the localization of poly(NIPAM) nanoparticles *within* the skin, the notion is supported by both the current MTX delivery and PGE_2 modulation data. Silver nanoparticles, 20–50 nm, have been demonstrated to penetrate the hair follicle and *stratum corneum*, reaching the viable epidermis, and these were successfully imaged in situ [27]; although they were some 3× smaller than the nanoparticles in the current work. However, other workers have as yet been unable to visualize nanoparticles within the skin [28], despite a growing body of evidence demonstrating enhanced fluxes from such structures [29,30]. Perhaps the most compelling evidence to date involves their location in the receptor phases of Franz diffusion cells, following the dosing onto skin of nanoparticles prepared from gold [31] and polyNIPAM [32].

In summary, a drug delivery system with a unique mechanism for topically applied MTX is proposed, comprised of a poly(NIPAM-*co*-BA) nanogel loaded with MTX that is capable of delivering the drug across the epidermis in levels that significantly reduce the biosynthesis of PGE_2, a key inflammation mediator. Both delivery and biological activity are significantly enhanced by the addition of Na_2CO_3, which was found not to be pro-inflammatory. In a therapeutic context, this MTX nanogel delivery system is potentially useful for the topical delivery of a drug that has presented significant challenges hitherto.

References

[1] G.D. Weinstein, J.L. McCullough, W.H. Eaglstein, A. Golub, R.C. Cornell, R.B. Stoughton, W. Clendenning, H. Zackheim, H.I. Maibach, K.R. Kulp, L. King, H.P. Baden, J.S. Taylor, D.D. Deneau, A clinical screening program for topical chemotherapeutic drugs in psoriasis, Arch. Dermatol. 117 (1981) 388–393.
[2] P. Collins, S. Rogers, The efficacy of methotrexate in psoriasis – a review of 40 cases, Clin. Exp. Dermatol. 17 (1992) 257–260.
[3] B. Eskicirak, E. Zemheri, A. Cerkezoglu, The treatment of psoriasis vulgaris: 1% topical methotrexate gel, Int. J. Dermatol. 45 (2006) 965–969.
[4] M.F. Ali, M. Salah, M. Rafea, N. Saleh, Liposomal methotrexate hydrogel for treatment of psoriasis: preparation, characterization and laser targeting, Med. Sci. Monit. 14 (2008) 66–74.
[5] T. Hellweg, Properties of NIPAM based intelligent microgel particles, in: L.M. Liz-marzan, P.V. Kamat (Eds.), Nanoscale Materials, Springer, New York, 2003, pp. 209–210.
[6] M. Das, H. Zhang, E. Kumcheva, Microgels: old materials with new applications, Annu. Rev. Mater. Res. 36 (2006) 117–142.
[7] B.R. Saunders, B. Vincent, Responsive microgel dispersion, in: P. Somasundaran, A. Hubbard (Eds.), Encyclopedia of Surface and Colloid Science, second ed., Taylor & Francis, New York, 2006, p. 5430.
[8] M.J. Murray, M.J. Snowden, The preparation, characterization and applications of colloidal microgels, Adv. Colloid Interface Sci. 54 (1995) 73–91.
[9] T. Hoare, R. Pelton, Highly pH and temperature responsive microgels functionalized with vinylacetic acid, Macromolecules 37 (7) (2004) 2544–2550.
[10] S. Neyret, B. Vincent, The properties of polyampholyte microgel particles prepared by microemulsion polymerization, Polymer 38 (25) (1997) 6129–6134.
[11] V. Kaneda, B. Vincent, Swelling behavior of PMMA-g-PEO microgel particles by organic solvents, J. Colloid Interface Sci. 274 (2004) 49–54.

[12] H. Zhang, S. Mardyani, W.C.W. Chan, E. Kumacheva, Design of biocompatible chitosan microgels for targeted pH-mediated intracellular release of cancer therapeutics, Biomacromolecules 7 (5) (2006) 1568–1572.
[13] V.C. Lopez, S.L. Raghavan, M.J. Snowden, Colloidal microgels as transdermal delivery systems, React. Funct. Polym. 58 (2004) 175–185.
[14] H.G. Schild, Poly(*N*-isopropylacrylamide): experiment, theory and application, Prog. Polym. Sci. 17 (1992) 163–249.
[15] www.cir-safety.org.
[16] M. Das, H. Zhang, E. Kumacheva, Microgels: old materials with new applications, Annu. Rev. Mater. Res. 36 (2006) 117–142.
[17] R. Pelton, Temperature-sensitive aqueous microgels, Adv. Colloid Interface Sci. 85 (2000) 1–33.
[18] I. Galaev, B. Mattiasson, Smart polymers – applications in biotechnology and biomedicine, second revision, Taylor & Francis Ltd., Boca Raton, 2007.
[19] G.A. Simon, H.I. Maibach, The pig as an experimental animal model of percutaneous permeation in man: qualitative and quantitative observations – an overview, Skin Pharmacol. Appl. 13 (2000) 229–234.
[20] U. Jacobi, M. Kaiser, H. Richter, H. Audring, W. Sterry, J. Lademann, The number of stratum corneum cell layers correlates with the pseudo-absorption of the corneocytes, Skin Pharmacol. Physiol. 18 (2005) 175–179.
[21] M.H. Zulfakar, C.M. Heard, Enhanced topical delivery and ex vivo antiinflammatory activity from a betamethasone dipropionate formulation containing fish oil, Inflamm. Res. 59 (2010) 23–30.
[22] J. Brijitta, B.V.R. Tata, T. Kaliyappan, Phase behavior of poly(*N*-isopropylacrylamide) nanogel dispersions: temperature dependent particle size and interactions, J. Nanosci. Nanotechnol. 9 (2008) 5323–5328.
[23] B.R. Saunders, N. Laajam, E. Daly, S. Teow, X. Hu, X.R. Stepto, Microgels: from responsive polymer colloids to biomaterials, Adv. Colloid Interface Sci. 147–148 (2008) 251–262.
[24] L.H. Gracia, M.J. Snowden, Preparation, properties and applications of colloidal microgels, in: P.A. Williams (Ed.), Handbook of Industrial Water Soluble Polymers, Blackwell Publishing, Oxford, 2007, pp. 268–297.
[25] I.Y. Galeaev, B. Mattiasson, Smart polymers – applications in biotechnology and biomedicine, vol. 1, second revision, Taylor & Francis, Boca Raton, 2007.
[26] N.A. Megrab, A.C. Williams, B.W. Barry, Estradiol permeation through human skin and silastic membrane – effects of propylene-glycol and supersaturation, J. Control. Release 36 (1995) 277–294.
[27] F.F. Larese, F. D'Agostin, M. Crosera, G. Adami, N. Renzi, M. Bovenzi, M.G. Maina, Human skin penetration of silver nanoparticles through intact and damaged skin, Toxicology 255 (2009) 33–37.
[28] R. Alvarez-Román, A. Naik, Y.N. Kalia, R.H. Guy, Skin penetration and distribution of polymeric nanoparticles, J. Control. Release 99 (2004) 53–62.
[29] R. Alvarez-Román, A. Naik, Y.N. Kalia, R.H. Guy, H. Fessi, Enhancement of topical delivery from biodegradable nanoparticles, Pharm. Res. 21 (2004) 1818–1825.
[30] J.J. Wang, K.S. Liu, K.C. Sung, C.Y. Tsai, J.Y. Fang, Skin permeation of buprenorphine and its ester prodrugs from lipid nanoparticles: lipid emulsion, nanostructured lipid carriers and solid lipid nanoparticles, J. Microencapsul. 26 (2009) 734–747.
[31] S. Ganeshchandra, T. Keishiro, S. Akira, O. Hiroyuki, T. Hiroshi, M. Kimiko, In vitro permeation of gold nanoparticles through rat skin and rat intestine: effect of particle size, Colloids Surf. B: Biointerfaces 65 (2008) 1–10.
[32] N.H. Abu Samah, N. Williams, C.M. Heard. Nanogel particulates located within diffusion cell receptor phases following topical application demonstrates uptake into and migration across skin, Int. J. Pharm, in press.